

PAPER • OPEN ACCESS

Time-frequency characteristics of the strain signal of the metal shell under internal explosion

To cite this article: D Wei *et al* 2020 *J. Phys.: Conf. Ser.* **1507** 032071

View the [article online](#) for updates and enhancements.

You may also like

- [Understanding the nonlinear behavior of EEG with advanced machine learning in artifact elimination](#)
Md Samiul Haque Sunny, Shifat Hossain, Nashrah Afroze et al.
- [Phase-resolved Analyses of Millihertz Quasi-periodic Oscillations in 4U 1636-53 using the Hilbert–Huang Transform](#)
Hung-En Hsieh and Yi Chou
- [Signal denoising optimization based on a Hilbert-Huang transform-triple adaptable wavelet packet transform algorithm](#)
Fei Liu, Yongjun Zhang, Tanju Yildirim et al.



ECS
The
Electrochemical
Society
Advancing solid state &
electrochemical science & technology

DISCOVER
how sustainability
intersects with
electrochemistry & solid
state science research

Time-frequency characteristics of the strain signal of the metal shell under internal explosion

D Wei¹, Y D Gan^{1*}, Q M Zhang², J J Su¹, R R Long², P W Chen² and H Z Liang¹

¹ Xi'an Modern Chemistry Research Institute, Xi'an, Shanxi, 710065, China

² The State Key Lab of Explosion Science and Technology, Beijing Institute of Technology, Beijing, 100081, China

E-mail: ganyundan@163.com

Abstract. In this paper, the empirical mode decomposition-Hilbert Huang transform (EMD-HHT) was used to characterize the strain signal within metal cylindrical shell structure under internal blast loading. The received vibration frequencies of signal were closely consistent with FT characterization results. Through the EMD-HHT, instantaneous energy spectrum, marginal energy spectrum and Hilbert energy spectrum were determined, and these reflected the change in trend of signal energy in time domain, frequency domain, and time-frequency domain, showing the instantaneity and locality of explosion signal. The frequency components of the signal at any time were also determined, which proved that signals generated by the metal shell were the result of the superposition of different frequency signals under internal blast loading. This paper explains more clearly the time and frequency characteristics of blast signal, providing the theoretical basis for the study of antiknock in structures.

1. Introduction

Explosion vessels can limit the sphere of actions of shock waves and detonation products effectively, protect personnel and equipment, and facilitate observation of explosion and detonation processes. For this reason, explosion vessels are widely used in public security, national defense, and scientific research [1,2]. In recent years, some scholars have studied the explosion vessel strain signals. For example, Buzukou et al. were the first to discover the phenomenon of strain growth, and the cause of the phenomenon was concluded to be the energy transformation from breathing vibration energy into high frequency vibration of the container [3]. Zhu and Duffey suggested that modal superposition for vibration of similar frequency is the cause of the growth of strain signals [4,5]. Dong et al. indicated that the nonlinear coupling of breathing vibration modal and bending vibration modal was the chief reason for the increase in strain signal [6–8]. These research results were mainly concluded from the signal of time domain or frequency domain, which only somewhat indicated the characteristics of the combination with both time domain and frequency domain. Based on the existing research results, in this paper, the EMD-HHT was used to characterize the axial and hoop strain of the explosion vessel under internal blast loading of metal shell [9].

2. Strain signal acquisition

The explosion shockwave acts on the shell for only a short time, but the shell vibrates for much longer. In order to maintain the integrity of the recorded signal, the 3d digital image correlation method was used to measure strain signals generated by the action of the shockwave on the shell. As shown in figure 1, two high-speed cameras recorded speckle image information on surface of metal cylindrical



shells at different times. The displacement and deformation of the shell were determined by three-dimensional reconstruction according to the image information about grey correlation before and after the deformation [10,11]. This method involves non-contact measurement, avoiding interference of explosion charged gas during the measurement of resistance strain. In this way, it is a kind of high precision measurement [12,13]. The diameter and thickness of the metal cylindrical shell are 210 mm and 2.5 mm, respectively. Before the experiment, 10 g explosive (TNT) was put in the geometric center of the shell. The shooting rates of high-speed cameras were set to 100,000 frames per second. The strain information on the surface was obtained at different times through the speckle by the Vic-3d digital image correlation process. Figure 2(a) and (b) show the axial and hoop strain of the surface point P on the shell center section. As shown in figure 2(a), the baseline of axial strain vibrates at $y = 0$, showing that the axial deformation of the shell was within elastic range and that it was a stationary signal. Figure 2(b) shows that the hoop strain baseline increased sharply from $y = 0$ to $y = 2600$ at a certain point, indicating that the hoop deformation changed from an elastic to a plastic state, namely the signal mutation happened and that it was a non-stationary signal.

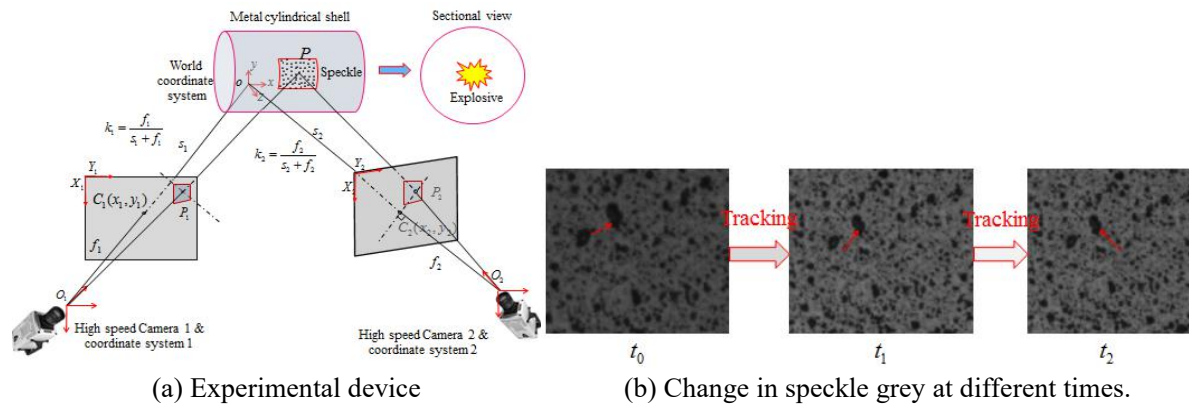


Figure 1. Experimental apparatus and test principles.

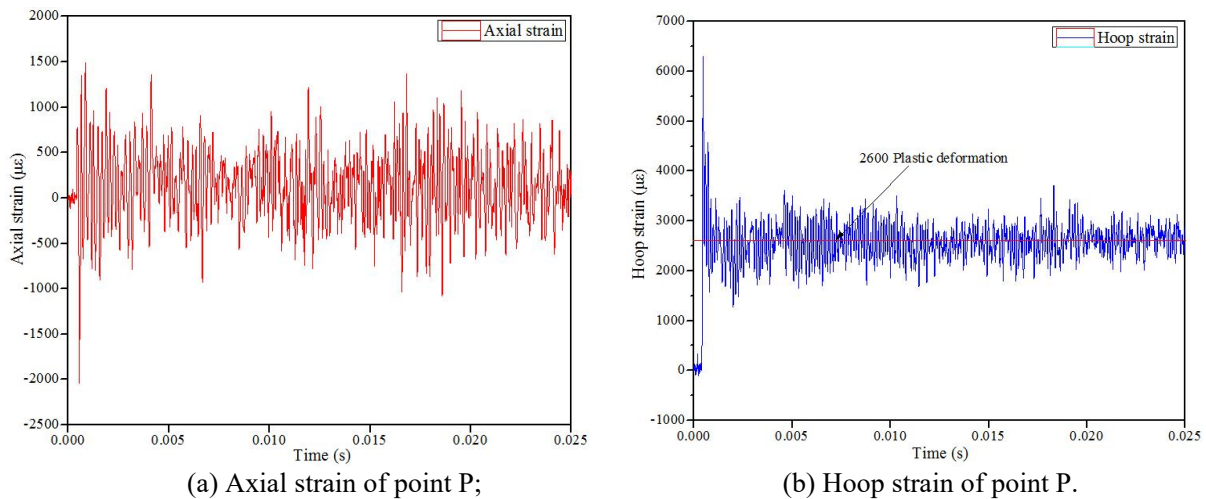


Figure 2. Axial and hoop strain of point P on the surface of the shell.

3. Strain signal representation

3.1. Signal FT

The characteristics of strain response were mainly visible in the time domain and frequency domain. The phenomena and rule, which were difficult to observe in time domain, sometimes were clearly shown in the frequency domain [14]. In this paper, the fast Fourier transform (FFT) of origin was used

in order to determine the time-frequency characteristics of the strain signal. Through FFT axial strain became a stationary signal, a basic function can represent the original signal. Then the frequency domain distribution was get, as shown in figure 3(a). Signals at 4886 Hz and 6579 Hz had greater amplitudes, while the moment of largest amplitude cannot be matched. This is because the FT is global transformation [15]. In other words, each frequency signal is produced by the performance of the system throughout the entire period, and the signal of each moment is also produced by the full frequency component performance. These signals cannot show the corresponding relationship between time domain signal and frequency domain signal at any moment. In this way, the signal lacks instantaneity. The frequency domain signal of hoop strain indicated by FFT is shown in figure. 3(b). The biggest deformation in the shell occurred at 0 Hz, but at 4886 Hz, 7518 Hz, and 8122 Hz, the amplitudes were smaller. In fact, 0 Hz was a static state. It contradicted the largest deformation state of the shell. This was because the FT, which was based on a linear, steady state and Gaussian assumption, could not use a single basic function to characterize non-stationary signal. The FT lacked the overall situation of the signal.

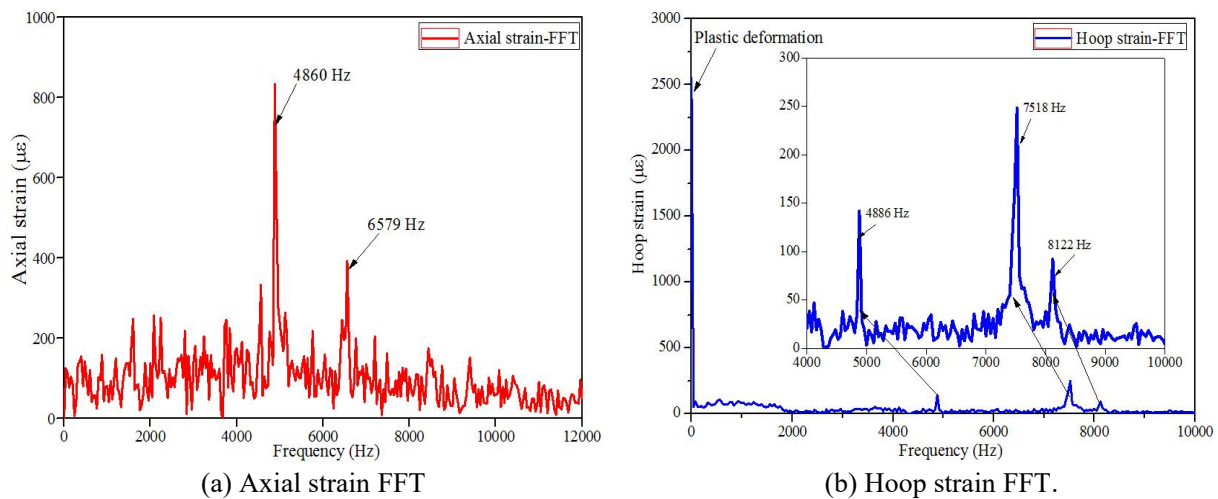


Figure 3. Corresponding FFTs of axial and hoop strain.

3.2. Signal EMD

EMD was used to overcome the shortfall of FT transforms. It decomposed the strain signal into fluctuations with different scales step by step, producing intrinsic mode function (IMF) with different scale characteristics. The method used in strain signal decomposition was the same as in previous works [9, 16]. The processes in MATLAB using EMD to deal with strain signal were as follows:

(1) Determine the extreme point of the signal. Use cubic spline function curve to construct the upper and lower envelope of signal. The difference between the strain signal $X(t)$ and the mean m_i of the top and bottom envelopes is defined as h_i .

$$h_i = X(t) - m_i \quad (1)$$

(2) h_i is served as a new signal $X(t)$ to repeat step (1). After k rounds of screening, when h_{1k} meets (2), it is denoted by IMF_1 . A difference signal r_i (residual) is obtained when IMF_1 is separated from $X(t)$. r_i served as a new signal for filtering until n iterations later, and when the differential signal r_n becomes a monotonic function, the signal decomposition becomes complete.

$$SD = \sum_{i=0}^T \left| \frac{h_{1(k-1)}(t) - h_{1(k)}(t)}{h_{1(k-1)}^2(t)} \right| = 0.25 \quad (2)$$

$$r_1 = X - IMF_1(t) \quad (3)$$

(3) The strain signal consists of n IMFs and a residual r_n . The IMFs contain the components of the original signal from high to low on different frequency bands. r_n represents the vibration trend of signals.

$$X(t) = \sum_{i=1}^n IMF_i(t) + r_n(t) \tag{4}$$

The strain signal is decomposed into eight IMFs with different scale characteristics by EMD. figure. 4(a–b) and (c–d) show the axial and hoop strain of the IMFs and the corresponding frequency obtained by EMD. The IMF1 and IMF2 of axial strain expressed dramatic changes in the time domain. The frequency amplitudes were large at 4883 Hz and 6543 Hz, and the IMF1 and IMF2 from hoop strain at 4883 Hz, 7520 Hz, and 7520 Hz vibrated more. These results were consistent with the results of FFT, indicating that the EMD can characterize the signal frequency domain information effectively.

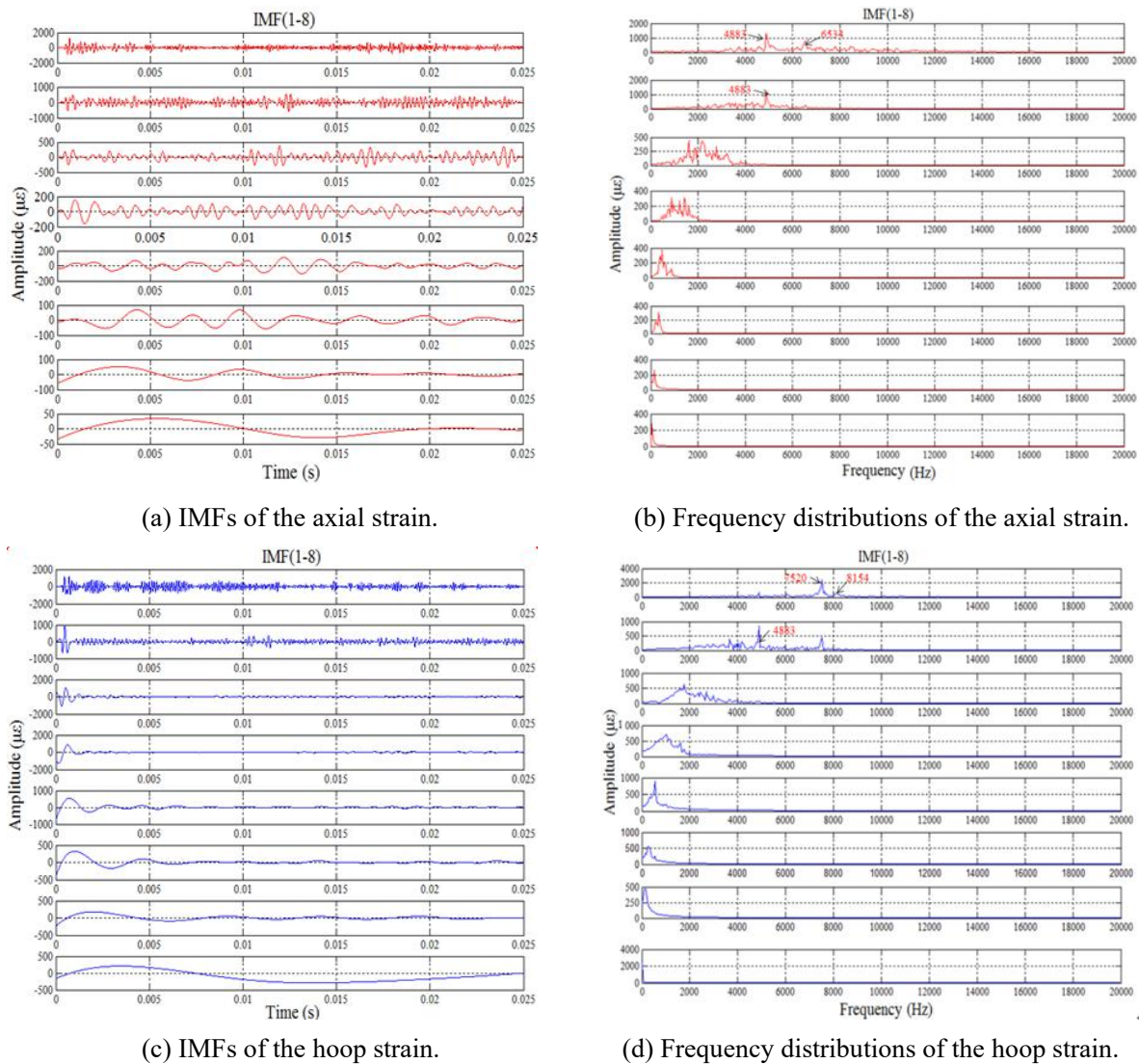


Figure 4. IMFs and frequency distributions of axial strain and hoop strain.

3.3. Signal HHT and representation

In order to represent the strain signal more clearly, the IMF obtained by EMD went to HHT. Then the strain signal amplitude can be indicated in the form of energy. The processes were as follows (5–11):

$$H[c(t)] = \frac{1}{\pi} PV \int_{-\infty}^{\infty} \frac{c(t')}{t-t'} dt' \quad (5)$$

$$z(t) = c(t) + jH[c(t)] = a(t) e^{j\Phi(t)} \quad (6)$$

$$f(t) = \frac{1}{2\pi} \omega(t) = \frac{d\Phi(t)}{dt} \quad (7)$$

$$H(\omega, t) = \text{Re} \sum_{i=1}^n a_i(t) e^{j\omega(t)dt} \quad (8)$$

$$IE(t) = \int_{\omega} H^2(\omega, t) d\omega \quad (9)$$

$$E(\omega) = \int_0^T H^2(\omega, t) dt \quad (10)$$

$$E(\omega, t) = \int_0^T H^2(\omega, t) dt \quad (11)$$

Among these, PV was the Cauchy principal value; $a(t) = \sqrt{c^2(t) + H^2[c(t)]}$ is amplitude function; $\Phi(t) = \tan^{-1} \frac{H[c(t)]}{c(t)}$ is the phase function; $f(t)$ is the instantaneous frequency; $H(\omega, t)$ is the Hilbert

spectrum; $IE(t)$, $E(\omega)$, and $E(\omega, t)$ are the instantaneous energy spectrum, marginal spectrum, and Hilbert spectrum, respectively; T is the signal period. For the HHT, there is a proportional factor between $IE(t)$, $E(\omega)$, $E(\omega, t)$ and the energy of the real physical space. Because the proportional factor was not involved in the calculation, its size and dimension could be ignored. $IE(t)$, $E(\omega)$, and $E(\omega, t)$ are not real energy. They only reflected the change tendency of energy.

The trend of axial strain energy in the time domain is shown in figure 5(a). The vibration of the shell structure under the blast loading can be divided into three stages: the initial stage of explosion shock wave action, the stage of shell inertia vibration, and the stage of reflected wave action. Figure 5(a) clearly shows these three stages (I, II, and III). The action time of the first stage was short, with the maximum instantaneous energy; during the second stage, the shell vibrates with the inertial effect. This stage was not affected by other factors, and the instantaneous energy reached the minimum; during the third stage, the explosion gas was reflected by the wall and then re-acting on the shell. Because the speed of gas expansion was decaying, the kinematic velocity of gas in this stage was smaller than in the initial stage, leading less energy acts on the shell. The relative energy of the three stages were 30.08%, 27.22%, and 41.94%, respectively. Figure 5(b) shows the changing trends of axial strain energy in the frequency domain. The signal changes drastically at frequencies of 4000–6500 Hz, which accounted for 68.07% of total energy. The proportion of energy below 4000 Hz was 16.41% and above 6500 Hz frequency was 15.52% of the whole frequency band. The Hilbert spectrum is shown in figure 5(c), indicates changes in the energy in the time domain and frequency domain. It also shows the signal amplitude in a certain period of time within a certain frequency band, indicating the instantaneity and locality of signals.

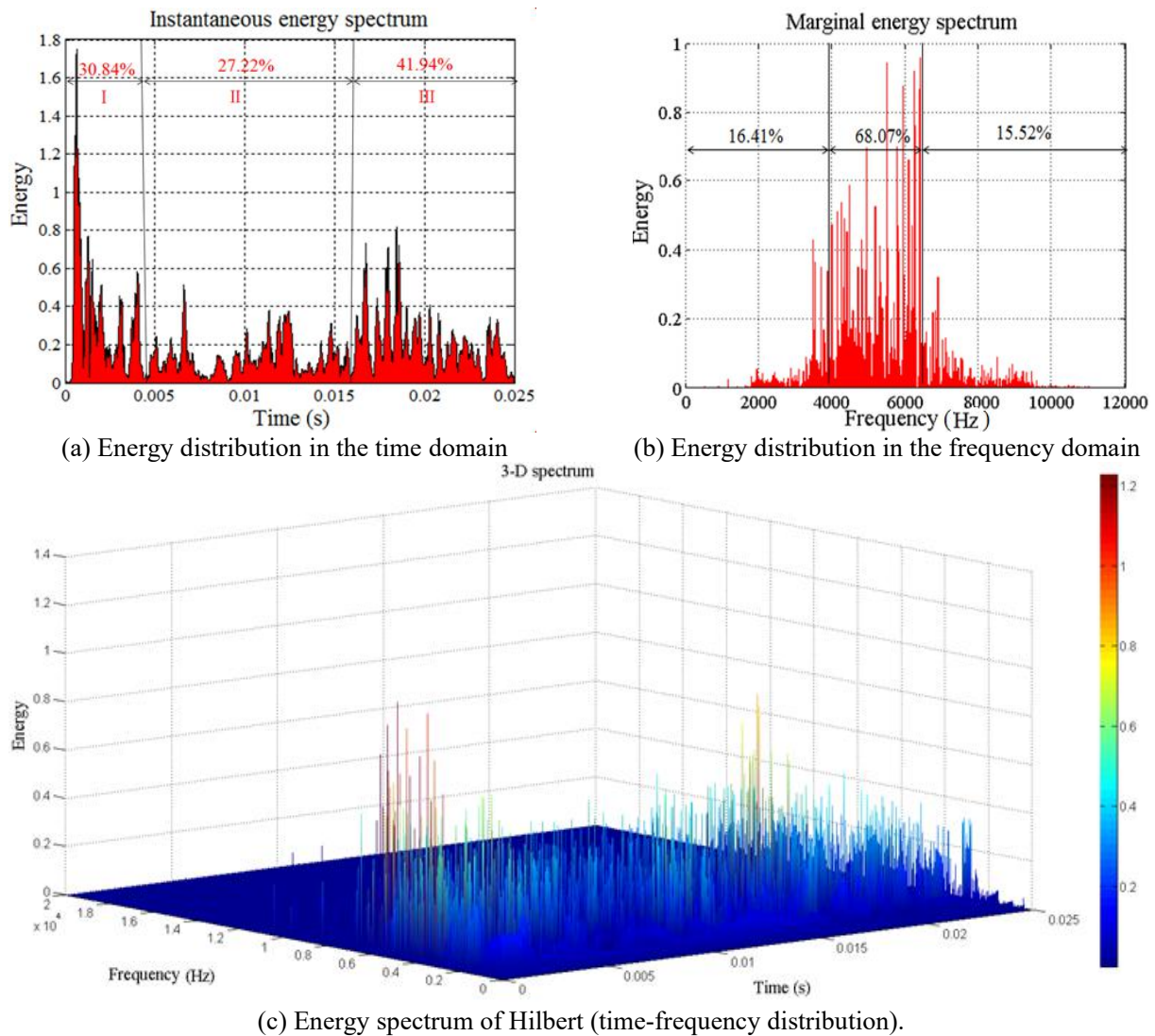


Figure 5. Energy distributions in time domain, frequency domain, and time-frequency domain distribution of axial strain.

Changing trends of hoop strain energy in the time domain is shown in figure 6(a). The changing trend of instantaneous energy is divided into two parts. The instantaneous energy before 0.0075 s accounted for 54.86% of the whole period of signal energy. During this stage, the hoop of the shell undergoes plastic deformation and absorbs most energy carried by the explosion’s shockwave. Figure 6(b) shows the trends in hoop strain energy in the frequency domain. Here, 0–2200 Hz accounted for 64.14% of the whole frequency domain energy, and the energy ratio above 2200 Hz frequency accounted for only 35.86%. Figure 6(c) shows the Hilbert spectrum, namely the change trend of hoop strain energy in the time-frequency domain. As shown, the hoop plastic deformation of shell occurred before 0.005 s and below 5000 Hz. It is the time and frequency that match the plastic deformation.

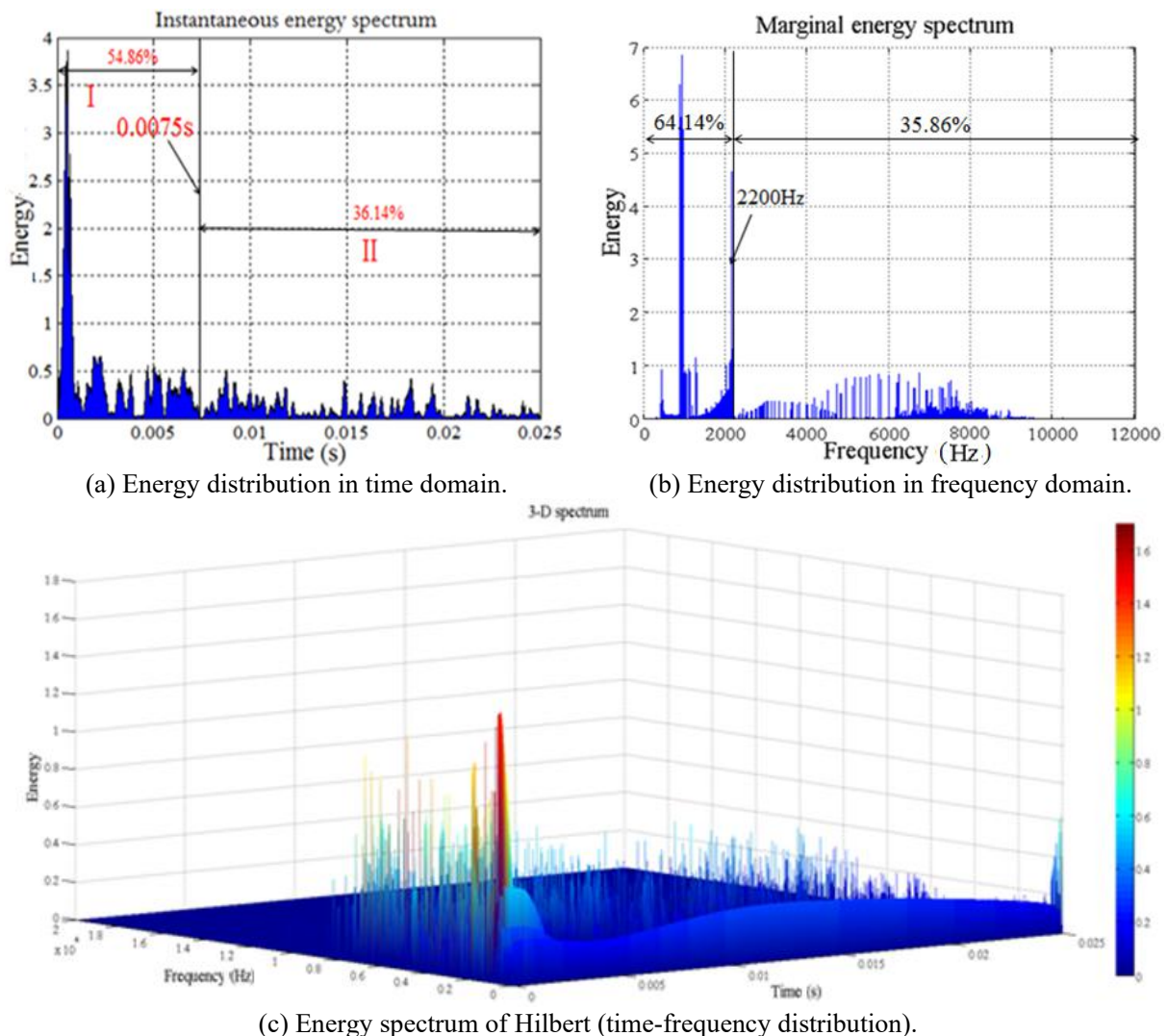


Figure 6. Energy distributions in time domain, frequency domain, and time-frequency domain distribution of hoop strain.

3.4. Instantaneous signal frequency distribution

Figure 5(c) and 6(c) show the signal at a particular instant, including abundant frequency message, which contains not only low frequency component but also high frequency component. In order to study the transient signal frequency components, frequency at any moment and frequency at the moment of maximum energy were selected for further analyzing. Figure 7(a) and (b) show the frequency components from axial strain signals at any moment and at the moment of largest instantaneous energy, respectively. At each moment there were four frequency components, among which high frequency component accounted for most of the instantaneous energy (high frequency components were defined relative to the low frequency at the same time). As shown in the figure, the elastic energy signal was found to consist mainly of the high-frequency energy signal. As shown in figure 7(c–d), the hoop strain frequency was found to consist mainly of the low-frequency component (that is, the hoop plastic deformed in low frequency band). Figure 7(a–b) and (c–d) show the frequency components of the plastic signal frequency to be richer than the component of the elastic signal frequency. At the same time, results demonstrated that the strain signal of shell under explosion loading to overlap different frequency signals.

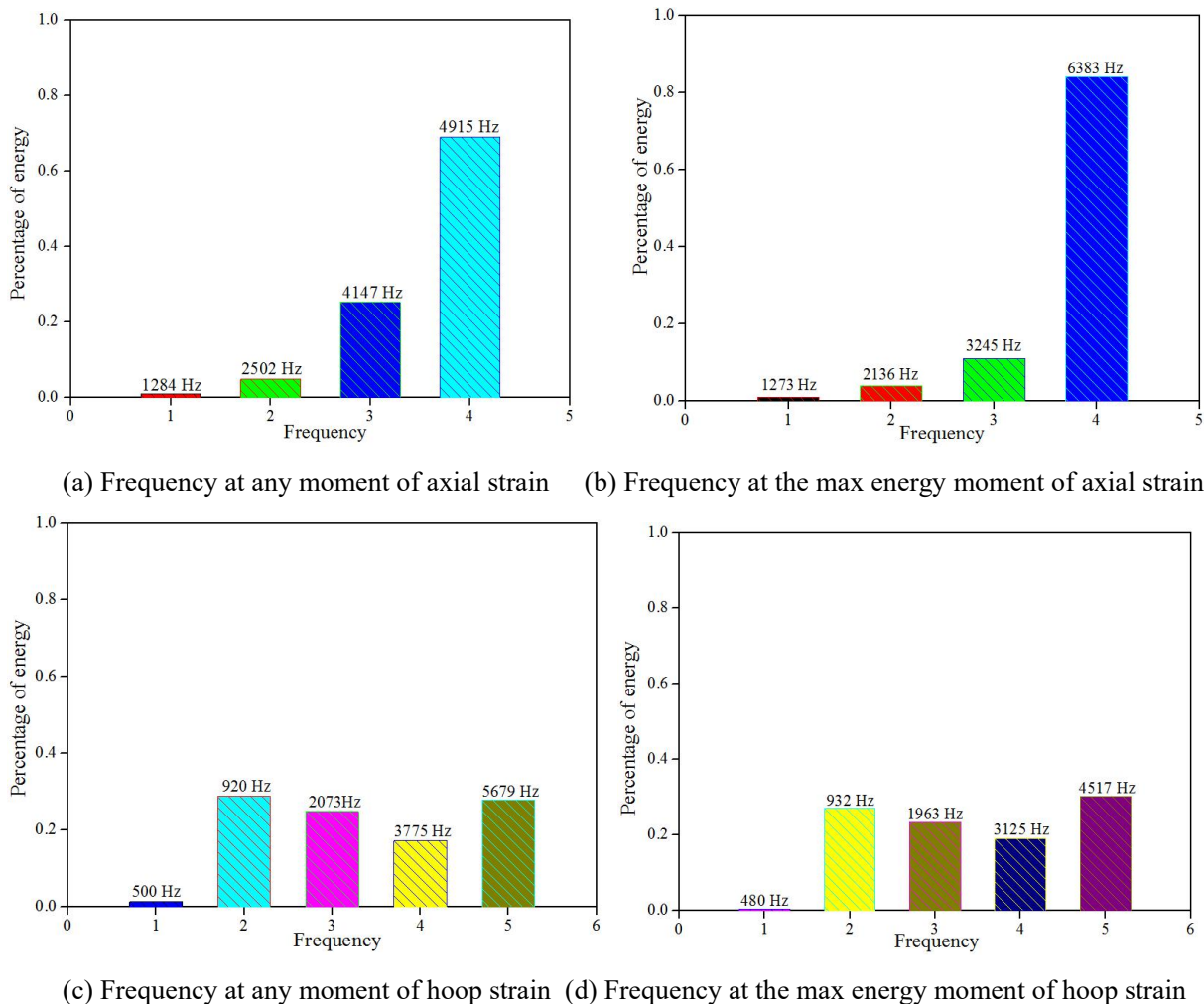


Figure 7. Frequency of axial strain and the hoop strain at any moment and at the max energy moment.

4. Conclusion

In conclusion, the frequency of the signal acquired by the EMD was here found to be closely consistent with FFT characterization results, demonstrating the effectiveness of EMD method in the characterization of the signal. The IMF through HHT received the changing trend of signal energy in time domain, frequency domain, and time-frequency domain, leading to the good characterization of the instantaneity and locality of signals. The signal at a particular component of the instantaneous frequency was determined. The results show that the elastic deformation (signal) is mainly composed of high-frequency components, and plastic deformation occurred at low frequencies. It also demonstrated the strain signal of shell under explosion loading to be overlapped by different frequency signals. This study paves the way for further understanding of the time-frequency characteristics of explosion signal and the changes in time and frequency of the energy carrying by signals. These results provide a theoretical basis for the study of anti-knocking.

References

- [1] Zhao S D. 1989 *Explosion and shock waves* **9** 85-96
- [2] Zhu W H, Xue H L, Han J W and Liu G Z. 1996 *Advances in mechanics* **26** 68-77
- [3] Buzukov A A. 1976 *Combust. Explo. Shock* **12** 549-54
- [4] Zhu W H, Xue H L and Han J W. 1997 *Int. J. Impact Eng.* **19** 831-45

- [5] Duffey T A and Romero C. 2003 *Int. J. Impact Eng.* **28** 967-83
- [6] Li Q M, Dong Q and Zheng J Y. 2008 *Int. J. Impact Eng.* **35** 1130-53
- [7] Dong Q, Li Q M and Zheng J Y. 2009 *Int. J. Impact Eng.* **35** 1-10
- [8] Dong Q, Li Q M and Zheng J Y. 2010 *Int. J. Impact Eng.* **37** 196-206
- [9] Yang Y F and Wu Y F. 2013 *Application of empirical mode decomposition in vibration analysis*(National Defense Industry Press)
- [10] Huang N E, Shen Z and Long S R. 1998 *Nonlinear and non-stationary time series analysis* **454** 903-95
- [11] Tiwari V, Sutton M A and McNeill S R. 2009 *Int. J. Impact Eng.* **36** 862-74
- [12] Wang W Z, Mottershead J E and Sebastian C M. 2011 *Int. J. Solids Struct.* **48** 1644-57
- [13] Yao X F, Jin J C and Ye H Y. 2005 *Polym. Test.* **24** 245-51
- [14] Jerabek M, Major Z and Lang R W. 2010 *Polym. Test.* **29** 407-16
- [15] Peng Z K, Tse P W and Chu F L. 2005 *J. Sound Vib.* **286** 187-205
- [16] Yu D J, Cheng J S and Yang Y. 2005 *Mech. Syst. and Signal Pr.* **19** 259-70